r3_cmc: Three-Terminal Nonlinear (Diffused and Poly-Silicon) Resistor Model and JFET Model

Revision History

Version	Date	Authors	Comments
1.0.0	06/12/2007	C. C. McAndrew	Initial release.

Review History

Revision	Date	Reviewers

Table of Contents

1 Introduction

The `r3_cmc` model is a nonlinear 3-terminal resistor model that includes self-heating, velocity saturation, statistical variations, and parasitic capacitances and currents. The core depletion pinching model formulation is for *p-n* junctions of diffused resistors, but is also applicable for the MOS behavior of polysilicon resistors. As *p-n* junction depletion pinching controls JFET device behavior, the `r3_cmc` model is also applicable to JFETs.

NOTE: in this documentation parameters are set in `Courier New` font, to distinguish them from other quantities.

2 Usage

(NOTE: exact usage may be simulator dependent; e.g. whether the local temperature rise node for self-heating is made available or not, and whether the initial instance key-letter "`r`" is required.)

```
r<instanceName> (<n1> <nc> <n2>) <modelName> <instanceParameters>
.model <modelName> r3_cmc <modelParameters>
```
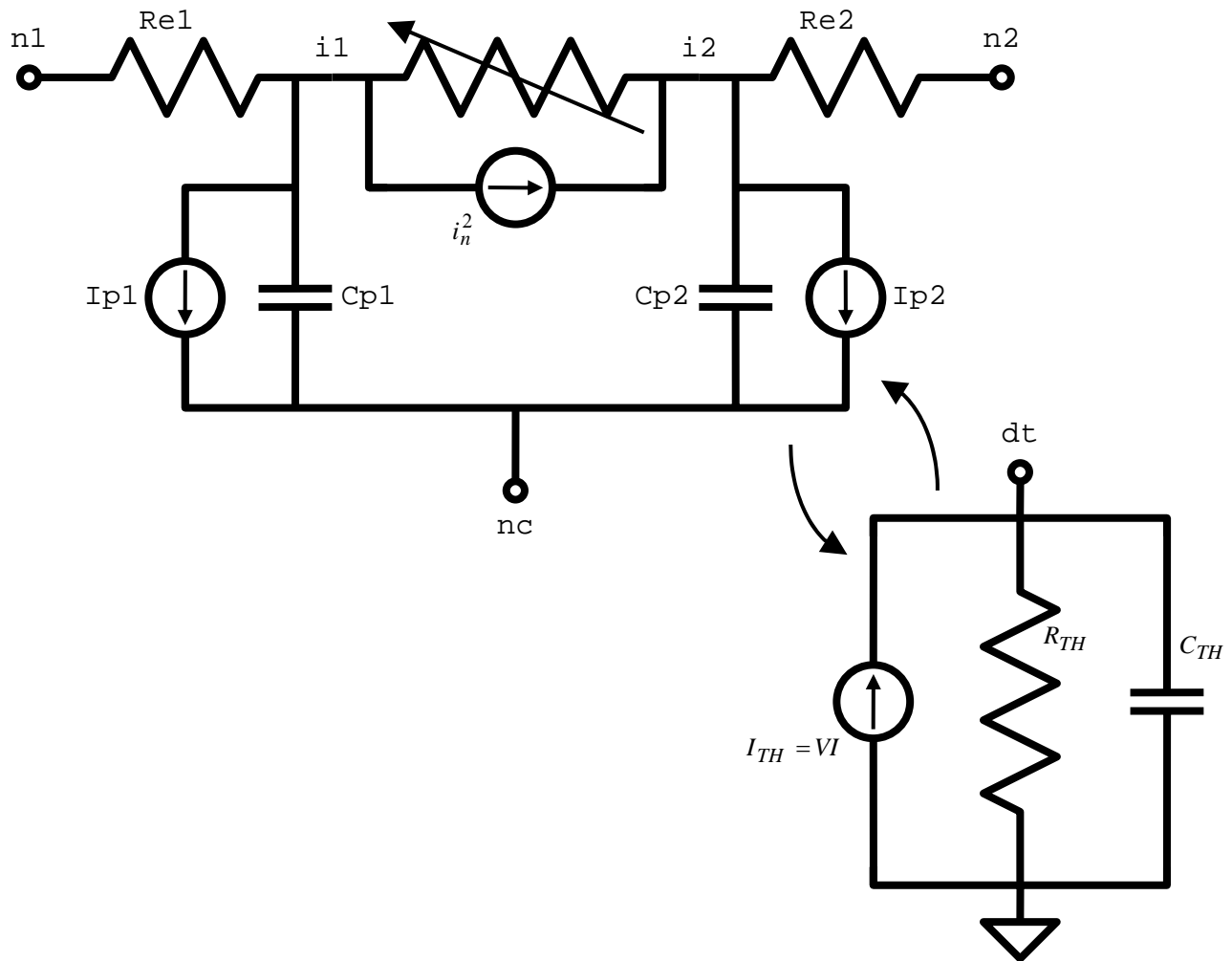

Fig. 1 `r3_cmc` Model Equivalent Network.

3   Instance Parameters

Name	Default	Min.	Max.	Units	Description
m	1	0	inf		multiplicity factor (number in parallel)
w	1.0e-6	0.0	inf	m	design width of resistor body
l	1.0e-6	0.0	inf	m	design length of resistor body
wd	0.0	0.0	inf	m	dogbone width (total; not per side)
a1	0.0	0.0	inf	m^2	area of node n1 partition
p1	0.0	0.0	inf	m	perimeter of node n1 partition
c1	0	0	inf		# contacts at n1 terminal
a2	0.0	0.0	inf	m^2	area of node n2 partition
p2	0.0	0.0	inf	m	perimeter of node n2 partition
c2	0	0	inf		# contacts at n2 terminal
trise	0.0			°C	local temperature delta to ambient (before self-heating)
sw_noise	1	0	1		switch for including noise: 0=no 1=yes
sw_et	1	0	1		switch for turning off self-heating: 0=exclude 1=include
sw_mman	0	0	1		switch for mismatch analysis: 0=no and 1=yes
nsmm_rsh	0.0				number of standard deviations of local variation for rsh
nsmm_w	0.0				number of standard deviations of local variation for w
nsmm_l	0.0				number of standard deviations of local variation for l

Table 1 Instance Parameters
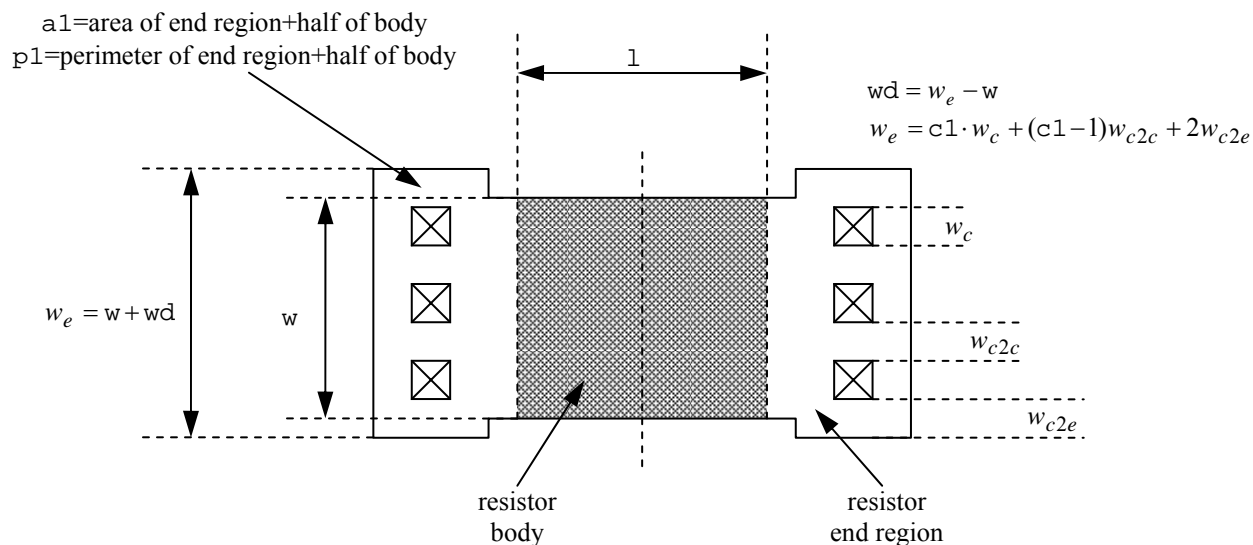
Fig. 2 Instance Parameter examples, note that the end region dogbone may be asymmetric.

4 Special Model Parameters

Name	Default	Min.	Max.	Units	Description
version					model version (major model change)
subversion					model subversion (minor model change)
revision					model revision (implementation update)
level	1003				model level
type	−1	−1	+1		resistor type: −1=n-body and +1=p-body
scale	1.0	0.0	1.0		scale factor for instance geometries
shrink	0.0	0.0	100.0	%	shrink percentage for instance geometries
tmin	−100.0	−250.0	27.0	°C	minimum ambient temperature
tmax	500.0	27.0	1000.0	°C	maximum ambient temperature
rthresh	0.001	0.0	inf	Ω	threshold to switch end resistance to V=I*R form
gmin	1.0e-12	0.0	inf	S	minimum conductance (for parasitic branches)
imax	1.0	0.0	inf		current at which to linearize diode currents
lmin	0.0	0.0	inf	µm	minimum allowed drawn length
lmax	9.9e99	lmin	inf	µm	maximum allowed drawn length
wmin	0.0	0.0	inf	µm	minimum allowed drawn width
wmax	9.9e99	wmin	inf	µm	maximum allowed drawn width
jmax	100.0	0.0	inf	A/um	maximum current density
vmax	9.9e99	0.0	inf	V	maximum voltage w.r.t. control node nc
tminclip	−100.0	−250.0	27.0	°C	clip minimum temperature
tmaxclip	500.0	27.0	1000.0	°C	clip maximum temperature

Table 2 Special Model Parameters

5 Model Parameters

Name	Default	Min.	Max.	Units	Description
tnom	27.0	-250.0	1000.0	°C	nominal (reference) temperature
rsh	100.0	0.0	inf	$\Omega/\square$	sheet resistance
xw	0.0			μm	width offset (total)
nwxw	0.0			μm^2	narrow width width offset correction coefficient
wexw	0.0			μm	webbing effect width offset correction coefficient (for dog-boned devices)
fdrw	1.0	0.0	inf	μm	finite doping width offset reference width
fdxwinf	0.0			μm	finite doping width offset width value for wide devices
xl	0.0			μm	length offset (total)
xlw	0.0				width dependence of length offset
dxlsat	0.0			μm	additional length offset for velocity saturation calculation
nst	1.0	0.1	5.0		subthreshold slope parameter
ats	0.0	0.0	inf	V	saturation smoothing parameter
dfinf	0.01	0.0001	10.0	$/\sqrt{V}$	depletion factor for wide/long device
dfw	0.0			$\mu m/\sqrt{V}$	depletion factor 1/w coefficient
dfl	0.0			$\mu m/\sqrt{V}$	depletion factor 1/l coefficient
dfwl	0.0			$\mu m^2/\sqrt{V}$	depletion factor 1/(w*l) coefficient
sw_dfgeo	1	0	1		switch for depletion factor geometry dependence: 0=drawn and 1=effective
dp	2.0	0.1	1000.0	V	depletion potential
ecrit	4.0	0.02	1000.0	V/μm	velocity saturation critical field
ecorn	0.4	0.01	ecrit	V/μm	velocity saturation corner field
du	0.02	0.0	1000.0		mobility reduction at ecorn
rc	0.0	0.0	inf	Ω	resistance per contact
rcw	0.0	0.0	inf	$\Omega\mu m$	width adjustment for contact resistance
fc	0.9	0.0	0.99		depletion capacitance linearization factor
isa	0.0	0.0	inf	$A/\mu m^2$	diode saturation current per unit area
na	1.0	0.0	inf		ideality factor for isa
ca	0.0	0.0	inf	$F/\mu m^2$	fixed capacitance per unit area
cja	0.0	0.0	inf	$F/\mu m^2$	depletion capacitance per unit area
pa	0.75	0.0	inf	V	built-in potential for cja
ma	0.33	0.0	1.0		grading coefficient for cja
aja	-0.5			V	smoothing parameter for cja

Name	Default	Min.	Max.	Units	Description
isp	0.0	0.0	inf	A/ μm	diode saturation current per unit perimeter
np	1.0	0.0	inf		ideality factor for isp
cp	0.0	0.0	inf	F/μm	fixed capacitance per unit perimeter
cjp	0.0	0.0	inf	F/μm	depletion capacitance per unit perimeter
pp	0.75	0.0	inf	V	built-in potential for cjp
mp	0.33	0.0	1.0		grading coefficient for cjp
ajp	-0.5			V	smoothing parameter for cjp
vbv	0.0	0.0	inf	V	breakdown voltage
ibv	1.0e-6	0.0	inf	A	current at breakdown
nbv	1.0	0.0	inf		ideality factor for breakdown current
kfn	0.0	0.0	inf		flicker noise coefficient (unit depends on afn)
afn	2.0	0.0	inf		flicker noise current exponent
bfn	1.0	0.0	inf		flicker noise 1/f exponent
sw_fngeo	0	0	1		switch for flicker noise geometry calculation: 0=drawn 1=effective
ea	1.12			V	activation voltage for diode temperature dependence
xis	3.0				exponent for diode temperature dependence
tc1	0.0			/K	resistance linear TC
tc2	0.0			/K^2	resistance quadratic TC
tc1l	0.0			μm /K	resistance linear TC length coefficient
tc2l	0.0			μm /K^2	resistance quadratic TC length coefficient
tc1w	0.0			μm /K	resistance linear TC width coefficient
tc2w	0.0			μm /K^2	resistance quadratic TC width coefficient
tc1rc	0.0			/K	contact resistance linear TC
tc2rc	0.0			/K^2	contact resistance quadratic TC
tc1kfn	0.0			/K	flicker noise coefficient linear TC
tc1vbv	0.0			/K	breakdown voltage linear TC
tc2vbv	0.0			/K^2	breakdown voltage quadratic TC
tc1nbv	0.0			/K	breakdown ideality factor linear TC
gth0	1.0e+6	0.0	inf	W/K	thermal conductance fixed component
gthp	0.0	0.0	inf	W/Kμm	thermal conductance perimeter component
gtha	0.0	0.0	inf	W/Kμm^2	thermal conductance area component
gthc	0.0	0.0	inf	W/K	thermal conductance contact component
cth0	0.0	0.0	inf	sW/K	thermal capacitance fixed component
cthp	0.0	0.0	inf	sW/Kμm	thermal capacitance perimeter component

Name	Default	Min.	Max.	Units	Description
ctha	0.0	0.0	inf	sW/Kµm^2	thermal capacitance area component
cthc	0.0	0.0	inf	sW/K	thermal capacitance contact component
nsig_rsh	0.0				number of standard deviations of global variation for rsh
nsig_w	0.0				number of standard deviations of global variation for w
nsig_l	0.0				number of standard deviations of global variation for l
sig_rsh	0.0	0.0	inf	%	global variation standard deviation for rsh (relative)
sig_w	0.0	0.0	inf	µm	global variation standard deviation for w (absolute)
sig_l	0.0	0.0	inf	µm	global variation standard deviation for l (absolute)
smm_rsh	0.0	0.0	inf	%µm	local variation standard deviation for rsh (relative)
smm_w	0.0	0.0	inf	µm$^{1.5}$	local variation standard deviation for w (absolute)
smm_l	0.0	0.0	inf	µm$^{1.5}$	local variation standard deviation for l (absolute)
sw_mmgeo	0	0	1		switch for flicker noise geometry calculation: 0=drawn and 1=effective

Table 3 Model Parameters

6 Bias Dependence of Resistor Body Current

The `r3_cmc` model includes three basic forms of bias dependence. First, from the depletion (*p-n* junction or MOS) pinching of the conducting channel of the resistor. Second, from velocity saturation. And third, from self-heating.

The basic *p-n* junction depletion pinching bias dependence comes from the analysis of [1], with the simplification of [2] (which merges the vertical and lateral bias dependence into a single bias dependent form with geometry dependent parameters). The applicability of the same general form of bias dependence for poly resistors, where the MOS depletion effect pinches the resistor body, was shown in [3]. The fundamental form of the depletion pinching model is

(1) $\qquad I_{depl} = g V_{21}, \quad g = gf \cdot \left(1 - df \sqrt{dp + V_i}\right), \quad V_i = V_{21} + 2V_{1c}$

where $V_{21} = V(\texttt{i2}) - V(\texttt{i1})$ and $V_{1c} = V(\texttt{i1}) - V(\texttt{nc})$. Here dp is the depletion potential (which is just the model parameter $\texttt{dp}$), df is the depletion factor, and gf is the conductance factor; these are determined from instance and model parameters as detailed in the section on geometry dependence.

The velocity saturation model is from [2], and is a mobility reduction term that divides the conductance factor in (1). The model is smooth and symmetric, has value 1 when $V_{21} = 0$, and asymptotically approaches $1 + (E - \texttt{ecorn})/\texttt{ecrit}$ for large field $E = V_{21}/(leff\_um + \texttt{dxlsat})$ (*leff_um* is defined in the next section)

(2) $\qquad \mu_{red} = 1 + \sqrt{\left(\dfrac{E - E_{ce}}{2\,\texttt{ecrit}}\right)^2 + \dfrac{du\,E_{ce}}{\texttt{ecrit}}} + \sqrt{\left(\dfrac{E + E_{ce}}{2\,\texttt{ecrit}}\right)^2 + \dfrac{du\,E_{ce}}{\texttt{ecrit}}} - \sqrt{\left(\dfrac{E_{ce}}{2\,\texttt{ecrit}}\right)^2 + \dfrac{4\,du\,E_{ce}}{\texttt{ecrit}}}$

(see Fig. 3) where $E_{ce} = \sqrt{\texttt{ecorn}^2 + (2\,du \cdot \texttt{ecrit})^2} - 2\,du \cdot \texttt{ecrit}$.

The V_{21} used in the above expressions is smoothly limited so as not to exceed a saturation voltage V_{sat}, which is calculated as the V_{21} at which the output conductance becomes zero. To determine V_{sat} a slightly modified form of the velocity saturation model (2) is used (the asymptotic form noted above), that allows closed form solution and guarantees that any imprecision in calculation of V_{sat} is such that the output conductance at saturation is positive, so that there are no "wiggles" around the transition to saturation. The smooth transition is implemented via [2]

(3) $\qquad V_{21,eff} = \dfrac{2 V_{21} V_{sat}}{\sqrt{(V_{21} - V_{sat})^2 + 4\,\texttt{ats}^2} + \sqrt{(V_{21} + V_{sat})^2 + 4\,\texttt{ats}^2}}$

where $\texttt{ats}$ is a model parameter that controls the limiting. This limiting function differs from those often used in compact MOSFET models; it preserves symmetry. The control voltage used is also limited, to the pinch-off voltage

(4) $\qquad V_{1c,eff} = V_{po} - \texttt{nst} V_{tv} \ln\left(1 + \exp\left(\dfrac{V_{po} - V_{1c}}{\texttt{nst} V_{tv}}\right)\right), \quad V_{po} = \dfrac{1}{2df^2} - 0.5dp, \quad V_{tv} = kT/q.$

The self-heating affects the current through the temperature variation of the model parameters, primarily the sheet resistance. The current flowing between nodes `n2` and `n1` in Fig. 1 is then

(5) $\qquad I_{21} = I_{depl}/\mu_{red}.$
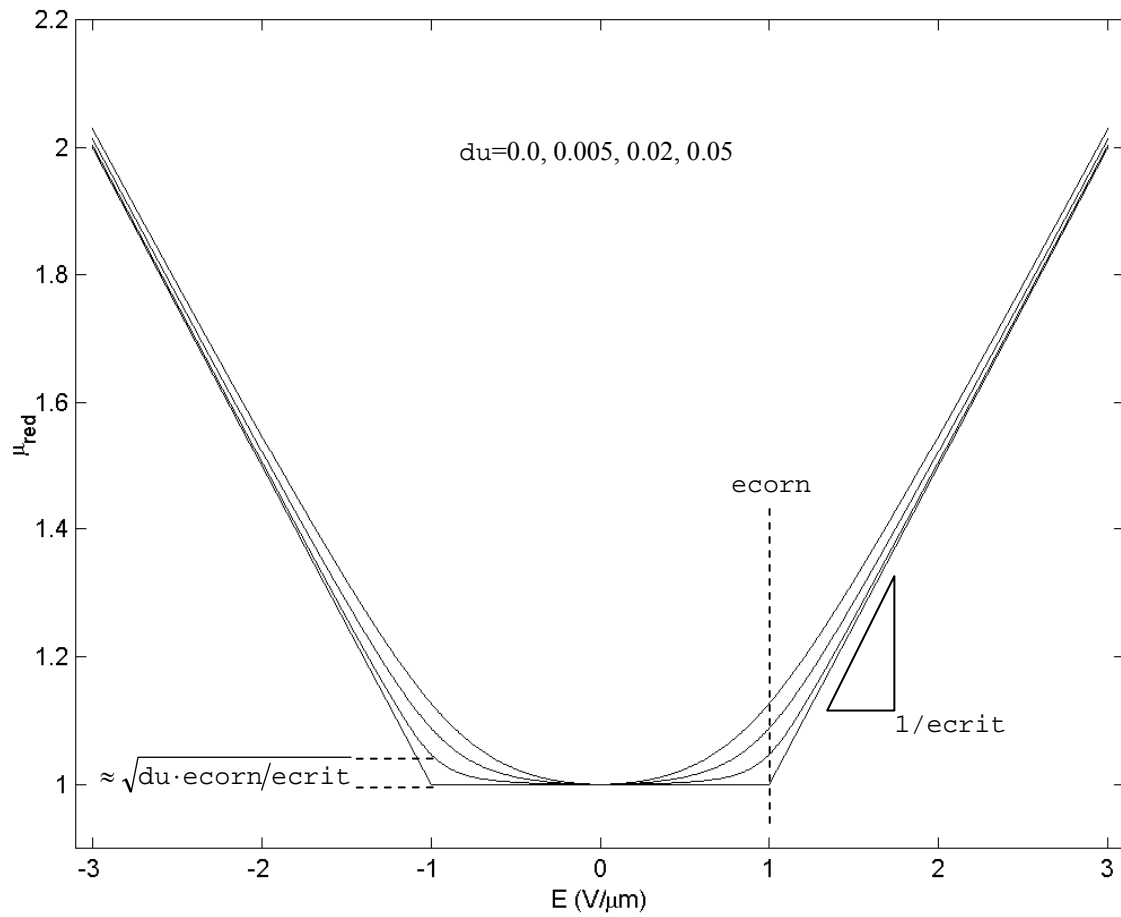
Fig. 3 Velocity saturation model.

7 Bias Dependence of Parasitics

The parasitic diode currents are

$$(6) \qquad I_{p1} = p1\_um \cdot I_{sp}(T)\big(\exp(V_{c1}/(\mathtt{np} \cdot V_{tv})) - 1\big) + a1\_um2 \cdot I_{sa}(T)\big(\exp(V_{c1}/(\mathtt{na} \cdot V_{tv})) - 1\big) + \mathtt{gmin} \cdot V_{gs}$$

$$(7) \qquad I_{p2} = p2\_um \cdot I_{sp}(T)\big(\exp(V_{c1}/(\mathtt{np} \cdot V_{tv})) - 1\big) + a2\_um2 \cdot I_{sa}(T)\big(\exp(V_{c2}/(\mathtt{na} \cdot V_{tv})) - 1\big) + \mathtt{gmin} \cdot V_{gd}$$

where $V_{c1} = V(\mathtt{nc}) - V(\mathtt{i1})$ and $V_{c2} = V(\mathtt{nc}) - V(\mathtt{i2})$. Each individual component of the diode currents is linearized for forward biases greater than the voltage at which the component is $\mathtt{imax}$. If there is no area or perimeter component of saturation current, then the minimum conductance terms are omitted. This is so there is no leakage current included for poly resistor modeling.

The breakdown currents, which are added to each parasitic current, are

$$(8) \qquad I_{b1} = -\mathtt{ibv}\big(\exp(-(V_{c1} + V_{bv}(T))/(n_{bv}(T)V_{tv})) - \exp(-V_{bv}(T)/(n_{bv}(T)V_{tv}))\big),$$

$$(9) \qquad I_{b2} = -\mathtt{ibv}\big(\exp(-(V_{c2} + V_{bv}(T))/(n_{bv}(T)V_{tv})) - \exp(-V_{bv}(T)/(n_{bv}(T)V_{tv}))\big)$$

and each of these is linearized for reverse biases greater than the voltage as which the magnitude of the current is $\mathtt{imax}$.

The parasitic capacitances comprise a bias independent component (intended for poly resistor modeling) and a bias dependent component (intended for diffused resistor modeling). The capacitances are implemented as bias dependent charges, but the resulting capacitances are given here,

$$(10) \qquad C_{p1} = p1\_um\left(\mathtt{cp} + \frac{C_{jp}(T)}{(1 - V_{c1}/P_p(T))^{\mathtt{mp}}}\right) + a1\_um2\left(\mathtt{ca} + \frac{C_{ja}(T)}{(1 - V_{c1}/P_a(T))^{\mathtt{ma}}}\right)$$

$$(11) \qquad C_{p2} = p2\_um\left(\mathtt{cp} + \frac{C_{jp}(T)}{(1 - V_{c2}/P_p(T))^{\mathtt{mp}}}\right) + a2\_um2\left(\mathtt{ca} + \frac{C_{ja}(T)}{(1 - V_{c2}/P_a(T))^{\mathtt{ma}}}\right).$$

The forward bias junction capacitance components are modified so that when the junction voltage (V_{c1} or V_{c2}) reaches $\mathtt{fc}$ multiplied by the associated built-in potential, the capacitance becomes linear in voltage, to avoid the singularity at the built-in potential. If the smoothing parameters $\mathtt{aja}$ and $\mathtt{ajp}$ are positive, then the transition from depletion to linear capacitance is done smoothly and not abruptly.

The thermal resistance and capacitance for the self-heating model are linear, and do not depend on temperature. The thermal power used for self-heating modeling is the sum of the powers of all dissipative (non-storage) elements in the equivalent circuit; i.e. the resistor body, the two end resistances, and two parasitic current sources.

8 Geometry Dependence

Unless otherwise noted, all `r3_cmc` model quantities scale with the multiplicity parameter `m` as defined in the Verilog-A Language Reference Manual (LRM), version 2.2.

The `r3_cmc` model includes several mechanisms for deviations of the effective electrical length and width of a resistor from the drawn (design, or mask) values. The drawn length and width of the resistor, in units of microns, are

$$(12) \qquad l\_um = \mathtt{l} \cdot \mathtt{scale} \cdot (1 - \mathtt{shrink}/100) \cdot 10^6 \,,$$

$$(13) \qquad w\_um = \mathtt{w} \cdot \mathtt{scale} \cdot (1 - \mathtt{shrink}/100) \cdot 10^6 \,.$$

Because subcircuit models for resistors can consist of multiple resistance sections connected in series, it is desirable to be able to switch on and off the "end corrections" for length to facilitate implementation of such multi-section models. This is the function of the `c1` and `c2` instance parameters of the `r3_cmc` model. The effective length offset is

$$(14) \qquad xleff = (\mathtt{xl} + \mathtt{xlw}/w\_um)((\mathtt{c1} > 0) + (\mathtt{c2} > 0))/2$$

(which is zero if neither end is contacted, $\mathtt{xl} + \mathtt{xlw}/w\_um$ if both ends are contacted, and one half of the latter if only one end is contacted). The effective electrical length, in microns, is

$$(15) \qquad leff\_um = l\_um + xleff \,.$$

For flexibility of separately fitting low bias resistance and velocity saturation, an additional offset `dxlsat` is added to $leff\_um$ for calculation of the electric field used in the velocity saturation model (2).

The effective width offset includes the physical effect models derived in [4]. These comprise a fixed offset for mask bias, lithography, and etching effects, and geometry dependent offsets for LOCOS, the webbing effect, and the finite dopant source effect. The effective electrical width, in microns, is

$$(16) \qquad weff\_um = \frac{w\_um + \mathtt{xw} + (\mathtt{nxw}/w\_um) + \mathtt{fdxwinf}(1 - \exp(-w\_um/\mathtt{fdrw}))}{1 - \mathtt{wexw} \cdot wd\_um/(l\_um \cdot w\_um)}$$

where the width of the dogbone (see Fig. 2), for the webbing effect model, in units of microns, is

$$(17) \qquad wd\_um = \mathtt{wd} \cdot \mathtt{scale} \cdot (1 - \mathtt{shrink}/100) \cdot 10^6 \,.$$

The depletion potential does not have a geometry dependence, so $dp = \mathtt{dp}$. The depletion factor depends on geometry as

$$(18) \qquad df = \mathtt{dfinf} + \frac{\mathtt{dfw}}{W} + \frac{\mathtt{dfl}}{L} + \frac{\mathtt{dfwl}}{WL}$$

where the width W and length L are effective geometries if `sw_dfgeo = 1` and design geometries otherwise (in units of micron).

The zero-bias resistance, which factors in the zero-bias depletion pinching, is then

$$(19) \quad R_0 = \mathtt{rsh} \frac{leff\_um}{weff\_um}\left(1.0 - df\sqrt{dp}\right), \quad gf = 1/R_0 \ .$$

Although end effects, such as spreading resistance and contact resistance, are assumed to be modeled via the `xl` parameter, the temperature coefficients of the end effects may differ from those of the body of the resistor. Simple analysis shows that these different temperature coefficients can be accounted for by introducing inverse length dependence to the temperature coefficients. A width dependence of temperature coefficients of resistance is also included in the model. Therefore in `r3_cmc`

$$(20) \quad T_{C1}^{eff} = \mathtt{tc1} + \frac{0.5\left((\mathtt{c1}>0)+(\mathtt{c2}>0)\right)\mathtt{tc1l}}{leff\_um} + \frac{\mathtt{tc1w}}{weff\_um} ,$$

$$(21) \quad T_{C2}^{eff} = \mathtt{tc2} + \frac{0.5\left((\mathtt{c1}>0)+(\mathtt{c2}>0)\right)\mathtt{tc2l}}{leff\_um} + \frac{\mathtt{tc2w}}{weff\_um}$$

where the length dependence is switched on, off, or halved, depending on whether the resistor is contacted at both ends, not contacted, or contacted at only one end, respectively. The dependence of the temperature coefficients on whether a resistor is contacted or not enables consistent modeling of temperature coefficients for single or multiple section models.

The thermal conductance and capacitance include area, perimeter, contact, and fixed components. Asymptotically for a large area device, the heat flow is perpendicular to the plane of heat generation in the resistor, and the heat energy stored in a device depends on its volume, hence the area dependent component. For a long resistor, as it becomes narrower more of the heat flow is conducted by a "fringe" path at the edges of the device, hence the perimeter dependent component. As both length and width decrease, the thermal conditions in the device asymptotically approach that of a point source in an infinite medium, hence the fixed component. Contacts conduct heat flow, hence the contact component. The thermal conductance and capacitance are therefore

$$(22) \quad g_{TH} = \mathtt{gth0} + \mathtt{gthp}\cdot p\_um2 + \mathtt{gtha}\cdot a\_um2 + \mathtt{gthc}\cdot(\mathtt{c1}+\mathtt{c2})$$

$$(23) \quad c_{TH} = \mathtt{cth0} + \mathtt{cthp}\cdot p\_um2 + \mathtt{ctha}\cdot a\_um2 + \mathtt{cthc}\cdot(\mathtt{c1}+\mathtt{c2})$$

where the area and perimeter are calculated as

$$(24) \quad a\_um2 = l\_um \cdot w\_um$$

$$(25) \quad p\_um = 2l\_um + \left((\mathtt{c1}>0)+(\mathtt{c2}>0)\right)w\_um \ .$$

The calculated perimeter therefore depends on whether the ends are contacted or not. Note that often the design dimensions of the body of a resistor differ from the overall dimensions of the device, for example if the design length is considered to be the unsalicided length of a poly resistor, the total resistor length will typically include silicided contact regions. So it is not readily apparent what dimension should be used in calculation of the thermal conductance and capacitance. That is why the design dimensions, rather than some effective dimensions (whose value is calculated to best fit DC electrical data), are used. This turns out to be reasonable (with the exception that differences between the perimeter components along length and width dimensions are ignored), because if there is some difference Δ between design and effective dimensions for thermal conductance modeling, then for a device contacted at both ends

$$(26) \quad \begin{aligned} g_{TH} &= \mathtt{gth0} + \mathtt{gthp}\left(2l\_um + 2w\_um + 4\Delta\right) + \mathtt{gtha}\left(l\_um+\Delta\right)\left(w\_um+\Delta\right) \\ &= \left(\mathtt{gth0} + 4\mathtt{gthp}\cdot\Delta + \mathtt{gtha}\cdot\Delta^2\right) + \left(\mathtt{gthp} + 0.5\mathtt{gtha}\cdot\Delta\right)p\_um + \mathtt{gtha}\cdot a\_um2 \end{aligned}$$

therefore any difference between design and effective dimensions can be taken into account by appropriate characterization of the fixed, perimeter, and area component parameters.

Because the "local" thermal conductance differs between the edge of a device and the center of a device, it is higher at the edge because of "fringing" conductance, the temperature of a resistor undergoing self-heating is not spatially uniform, but is lower at the edges than in the middle. This is not taken into account in the r3_cmc model.

The end resistances are calculated from the resistance per contact and the number of contacts (parallel to the width dimension; adding contacts parallel to the length dimension, which can be done for reliability purposes, does not alter the resistance much – unless the contact adjacent to the resistor body fails),

$$(27) \qquad R_{e1} = \frac{\texttt{rc} + \texttt{rcw}/w\_um}{\texttt{c1}}, \quad R_{e2} = \frac{\texttt{rc} + \texttt{rcw}/w\_um}{\texttt{c2}} .$$

The velocity saturation model includes geometry dependence in the bias dependent portion of the model evaluation, as it is formulated in terms of the electric field $E = V_{21} / (leff \_ um + \texttt{dxlsat})$.

The areas and perimeters of the end region partitions, used in parasitic calculations, are in units of microns

$$(28) \qquad p1\_um = \texttt{p1} \cdot \texttt{scale} \cdot (1 - \texttt{shrink}/100) \cdot 10^6 ,$$

$$(29) \qquad a1\_um2 = \texttt{a1} \cdot \left(\texttt{scale} \cdot (1 - \texttt{shrink}/100) \cdot 10^6 \right)^2 ,$$

$$(30) \qquad p2\_um = \texttt{p2} \cdot \texttt{scale} \cdot (1 - \texttt{shrink}/100) \cdot 10^6 ,$$

and

$$(31) \qquad a2\_um2 = \texttt{a2} \cdot \left(\texttt{scale} \cdot (1 - \texttt{shrink}/100) \cdot 10^6 \right)^2 .$$

If the number of contacts is not known, it can be calculated (see Fig. 2). Let the contact width (in the direction parallel to the resistor width) be w_c, the minimum spacing from a contact to the edge of the region it is in at the contact head of the resistor be w_{c2e}, and the (minimum) spacing between contacts be w_{c2c}. If (as in some older technologies) contacts can be scaled, then rc should be set to be the resistance of a minimum width contact and

$$(32) \qquad c[1,2] = \frac{\max(w + wd, w_c + 2w_{c2e}) - 2w_{c2e}}{w_c}$$

and for technologies where the contact width is fixed (assuming the maximum possible number of contacts are places)

$$(33) \qquad c[1,2] = \text{int}\left(\frac{\max(w + wd, w_c + 2w_{c2e}) - 2w_{c2e} + w_{c2c}}{w_c + w_{c2c}} \right) .$$

9 Temperature Dependence

The zero-bias resistance R_0 varies with temperature as

$$(34) \qquad R_0(T) = R_0 \left(1 + T_{C1}^{eff} \, dT + T_{C2}^{eff} \, dT^2 \right)$$

where R_0 is the nominal value of the zero-bias resistance (19) at the nominal temperature tnom, dT is the temperature difference (including self-heating) with respect to tnom, and T_{C1}^{eff} and T_{C2}^{eff} are first (linear) and second (quadratic) order effective temperature coefficients, from (20) and (21), respectively. Smooth limiting of the resistance temperature coefficient in (34) is implemented to a minimum value of 0.01. The conductance factor in (1) is then

$$(35) \qquad gf = 1/R_0(T).$$

The end resistances vary with temperature as

$$(36) \qquad R_{e[1,2]}(T) = R_{e[1,2]} \left(1 + \texttt{tc1rc} \cdot dT + \texttt{tc2rc} \cdot dT^2 \right)$$

and again the temperature coefficient in (36) is limited to a lower value of 0.01.

The parasitic diode saturation currents vary with temperature as

$$(37) \qquad I_{sa}(T) = \texttt{isa} \cdot rT^{\texttt{xis/na}} \exp\left(-\texttt{ea} \frac{1 - rT}{\texttt{na} \cdot V_{tv}} \right)$$

$$(38) \qquad I_{sp}(T) = \texttt{isp} \cdot rT^{\texttt{xis/np}} \exp\left(-\texttt{ea} \frac{1 - rT}{\texttt{np} \cdot V_{tv}} \right)$$

where rT is the ratio of device to nominal temperature (in Kelvin), and $V_{tv} = kT/q$ is the thermal voltage. The temperature dependence of the junction built-in potentials is

$$(39) \qquad P_a(T) = \texttt{pa} \cdot rT - 3V_{tv} \ln(rT) - \texttt{ea}(rT - 1)$$

$$(40) \qquad P_p(T) = \texttt{pp} \cdot rT - 3V_{tv} \ln(rT) - \texttt{ea}(rT - 1)$$

with a physically based modification to smoothly limit the potential to zero for high temperatures, and not allow it to become negative. The area and perimeter junction zero-bias capacitance temperature variations are

$$(41) \qquad C_{ja}(T) = \texttt{cja} \left(\frac{\texttt{pa}}{P_a(T)} \right)^{\texttt{ma}}$$

and

$$(42) \qquad C_{jp}(T) = \mathtt{cjp}\left(\frac{\mathtt{pp}}{P_p(T)}\right)^{\mathtt{mp}}.$$

The flicker noise coefficient varies with temperature as

$$(43) \qquad K_{FN}(T) = \mathtt{kfn}\left(1 + \mathtt{tc1kfn} \cdot dT\right)$$

where $\mathtt{kfn}$ and $\mathtt{tc1kfn}$ are model parameters (and the resulting K_{FN} is clipped to zero as a lower limit).

The breakdown voltage and ideality factor vary with temperature as

$$(44) \qquad V_{bv}(T) = \mathtt{vbv}\left(1 + \mathtt{tc1vbv} \cdot dT + \mathtt{tc2vbv} \cdot dT^2\right),$$

$$(45) \qquad n_{bv}(T) = \mathtt{nbv}\left(1 + \mathtt{tc1nbv} \cdot dT\right).$$

10 Noise

The noise model comprises two body components, a thermal (white) noise component and a flicker ($1/f$) noise component, thermal noise components for each contact resistance, and short noise components for each parasitic diode. These components are noise current spectral density (in A^2/Hz) that are implemented as a noise current sources in parallel with the associated element.

The thermal noise component of the resistor body is based on its DC conductance,

$$(46) \qquad i^2_{thermal,body} = 4kT_K G_{eff}(T)$$

where k is Boltzmann's constant, T_K is the device temperature (in Kelvin, including the effect of self-heating), and G_{eff} is the effective conductance of the resistor (at the temperature T). Similarly the thermal noise of each end resistances is

$$(47) \qquad i^2_{thermal,end} = 4kT_K/R_e(T) .$$

The flicker noise component is DC current dependent [5], and scales with geometry per the physical restrictions in [6],

$$(48) \qquad i^2_{flic\,ker,body} = K_{FN}(T)\left(\frac{I_{21}}{W}\right)^{\texttt{afn}} \frac{W}{L}\frac{1}{f^{\texttt{bfn}}}$$

where f is frequency (in Hz), `afn` and `bfn` are model parameters, $K_{FN}(T)$ is the temperature dependent flicker noise coefficient (43), I_{21} is the DC current in the resistor body (5), and W and L are the resistor width and length, respectively, in units of micron (μm). If the switch parameter for flicker noise geometry calculation `sw_fngeo` is 0 ("false") then W and L are design geometries, w_um and l_um respectively, else if it is 1 ("true") then W and L are effective geometries, $weff\_um$ and $leff\_um$ respectively.

The shot noise components are

$$(49) \qquad i^2_{shot,diode} = 2qI_{diode}$$

for each parasitic diode, where I_{diode} is the current in the diode.

Note that if self-heating is included, then possibly there is a frequency dependence to the flicker noise because of the thermal time constant. There is no data to verify this at present so a frequency independent noise current spectral density is used.

11 Operating Point Information

Name	Units	Description
v	V	voltage across resistor
ibody	A	current through resistor body
power	W	dissipated power
leff_um	μm	effective electrical length in μm
weff_um	μm	effective electrical width in μm
r0	Ω	zero-bias resistance
r_dc	Ω	DC resistance (including bias dependence)
r_ac	Ω	AC resistance (including bias dependence)
rth	K/W	thermal resistance
cth	sW/K	thermal capacitance
dt_et	K	self-heating temperature rise

Table 4 Operating Point Parameters

All flow and parameter quantities are for the overall device and include the effect of the multiplicity parameter m.

12 Statistical Variation

The `r3_cmc` model includes both global (inter-die, correlated between individual devices) and local (mismatch, uncorrelated between individual devices) variations. These can be added "on top" of a core model using sub-circuits, however this can involve increased complexity in model parameter files and increased computational overhead during simulation. Therefore statistical variation is "built-in" to the `r3_cmc` model, including instance parameters for control of mismatch variation for individual devices.

Besides convenience and efficiency, the statistical variation modeling in r3_cmc naturally embodies the geometry dependence of total variation in a device, which is not possible with statistical modeling based on a geometry independent global variation and geometry dependent correlation coefficients. And because it is based on independent statistical parameters for global variation and instance specific local variation, it does not require generation of correlated samples for distributional (i.e. Monte Carlo-like) simulation; if correlations were used then $N(N-1)/2$ of them are required for each statistical parameter for each of N devices.

Statistical variations are modeled in three parameters; the sheet resistance, the effective length variation, and the effective width variation. These are considered as the primary physical process parameters that determine the resistor behavior. At present there is no variation (global or local) in other physical quantities such as contact resistance, other parasitics (zero-bias depletion capacitance for diffused resistors varies with doping), or the parameters that control the nonlinearity of the model. If experimental data that show that linkage to more fundamental physical quantities, such as doping levels and layer thicknesses, is required to model correlations and statistical variations, this will be added in the future.

The local variation of the effective width is controlled by line edge roughness in the length dimension; its variance is therefore inversely proportional to the resistor length L. The local variation of the effective length is controlled by line edge roughness in the width dimension; its variance is therefore inversely proportional to the resistor width W. The local variation of the sheet resistance is controlled by random dopant fluctuations; its variance is therefore inversely proportional to the area of the resistor, WL. For flexibility in fitting experimental data, the `sw_mmgeo` flag allows the controlling geometries W and L to be either drawn or effective (as calculated before the statistical variations are applied, to avoid an implicit dependency that requires an iterative solution).

The total variance of a parameter is the sum of the variances of the global variance (which is independent of geometry) and the local variance (which depends on geometry $\vec{g}$, which can include area, width, and length),

(50) $$\sigma_{total}^2 = \sigma_{global}^2 + \sigma_{local}^2(\vec{g}).$$

Note that this naturally embodies the geometry dependence of the overall variance of a particular parameter. For statistical simulation, the perturbations of the global variation and the individual instance variation are expected to be statistically independent. But "proper" statistical simulation of a circuit requires inclusion of both global parameters and local parameters for every instance of a device type in a circuit. This can cause the number of statistical parameters included in a statistical simulation to increase proportionally with the number of devices in the circuit, with a concomitant explosion in the number of (local) statistical parameters needed to be included for a "proper" analysis. This is, for brute force statistical simulation, clearly impractical.

The `r3_cmc` model therefore includes a mechanism for more efficiently accounting for the geometry dependence of the overall variation. The `sw_mman` switch is provided to allow specification on an instance-by-instance basis of whether a device is being included in mismatch analysis. If yes, then both global and local (instance specific) statistical variation parameters are expected to be generated for each device instance, and the global and local variations are modeled separately. If no, which is appropriate for devices for which local variation is not expected to affect circuit performance, then the global variance for a device is adjusted to be the total variance for that device. This appropriately models the geometry dependent total variance for the device, with the consequence that it makes the total variation completely

correlated between all devices (that are not selected for individual mismatch analysis); this will cause overestimation of the variation of the circuit performances, i.e. the simulations from this will be pessimistic.

If mismatch analysis is selected, then the statistical variations are

$$(51) \qquad weff\_um = weff\_um_{nom} + \mathtt{nsig\_w} \cdot \mathtt{sig\_w} + \frac{\mathtt{nsmm\_w} \cdot \mathtt{smm\_w}}{\sqrt{\mathrm{m} \cdot L}}$$

$$(52) \qquad leff\_um = leff\_um_{nom} + \mathtt{nsig\_l} \cdot \mathtt{sig\_l} + \frac{\mathtt{nsmm\_l} \cdot \mathtt{smm\_l}}{\sqrt{\mathrm{m} \cdot W}}$$

$$(53) \qquad rsh = \mathtt{rsh}_{nom} \exp\left(0.01\left(\mathtt{nsig\_rsh} \cdot \mathtt{sig\_rsh} + \frac{\mathtt{nsmm\_rsh} \cdot \mathtt{smm\_rsh}}{\sqrt{\mathrm{m} \cdot WL}}\right)\right)$$

where the nominal values are those defined in the section on geometry dependence. (The above expressions are used to update the effective geometries and resistance values, and all previous model equations actually use the values calculated in (51) through (53), however for clarity of presentation and ease of interpretation the previous equations are not cluttered with the statistical variations).

Note that the variations in effective length and width are absolute, and are additive, and that the variation in sheet resistance is multiplicative. For small variations $\exp(x) \approx (1+x)$ hence the $\mathtt{rsh}$ variation is relative (it is more natural to think in terms of a % variation than an absolute variation). For large variations, as can be seen in some resistors, statistical sampling can generate very small or negative values of $\mathtt{rsh}$, which are unphysical. Quantities with large variations typically exhibit a log-normal distribution, and the exponential mapping in (53) transforms the normally distributed basic statistical parameters into a log-normal distribution for $\mathtt{rsh}$ if the variation is large. Note that strictly the unit "%" for the standard deviations of $\mathtt{rsh}$ is only for a small variation; if the variation is large then the exponential transformation in (53) modifies this.

This approach allows statistical modeling via uncorrelated normal variables, yet can capture log-normal distributions and correlations between parameters, via the dependencies on the fundamental process parameters that control the device behavior. Note that mismatch is modeled via independent perturbations in individual devices, which is physically correct. To simulate mismatch between two devices the mismatch instance parameters for both devices must be selected for statistical perturbation, and this easily extends to more than two devices, and implicitly accounts for geometry differences between different devices. If mismatch is characterized from differential measurements between two identically sized devices, then the measured standard deviations need to be divided by $\sqrt{2}$ when mapped into the model parameters $\mathtt{smm\_w}$, $\mathtt{smm\_l}$, and $\mathtt{smm\_rsh}$.

If mismatch analysis is not selected, then the total variance in (50) is used as the global variance,

$$(54) \qquad weff\_um = weff\_um_{nom} + \mathtt{nsig\_w}\sqrt{\mathtt{sig\_w}^2 + \mathtt{smm\_w}^2 / (\mathrm{m} \cdot L)}$$

$$(55) \qquad leff\_um = leff\_um_{nom} + \mathtt{nsig\_l}\sqrt{\mathtt{sig\_l}^2 + \mathtt{smm\_l}^2 / (\mathrm{m} \cdot W)}$$

$$(56) \qquad rsh = \mathtt{rsh}_{nom} \exp\left(0.01 \cdot \mathtt{nsig\_rsh}\left(\mathtt{sig\_rsh}^2 + \mathtt{smm\_rsh}^2 / (\mathrm{m} \cdot WL)\right)\right).$$

Note that the $\mathtt{nsig}$ parameters should be equated to global statistical variables in model files, as they are model parameters, not instance parameters. These parameters then should vary with case/corner and distributional simulations.

13 Notes on Parameter Extraction

This section provides some information that can help in setting up parameter extraction algorithms. It describes techniques to get initial values that can then be refined by optimization. It does not give a complete and perfect procedure for parameter extraction. As this section does not deal with the details of the model, but how to determine parameters from measured data, V and I will be used, in this section only, as the voltage across, and current through, the complete resistor (and not just the core resistor body, as is done in previous sections).

Techniques for extraction of basic parameters, such as `rsh`, `xl`, and `xw`, some temperature coefficients and their geometric scaling, etc. are provided in [7] and are not repeated here. Additional extraction techniques for the core bias dependence are provided here.

The fundamental depletion (*p-n* junction or MOS) pinching component of the model is given in (1). Velocity saturation and self-heating affect the bias dependence for $E = V/L$ significantly different from zero. Therefore the basic parameters of the model for one geometry, gf, df, and dp, should come from analysis of data where depletion pinching dominates, i.e. from low V, ideally extrapolated to, or measured (from small-signal AC excitation) at, $V = 0$. (The large signal conductance $g = I/V$ cannot be directly calculated at $V = 0$, but is equal to the small signal conductance $\partial I/\partial V$ at that bias).

There are at least three approaches to determine the basic depletion pinching parameters, for diffused resistors. If the conductance g from (1) is known from measurements at three different biases, then the parameters can be calculated as follows. For these biases ($V_i = V + 2V_{1c}$ for the ith values of V and V_{1c})

$$(57) \qquad g_i = gf\left(1 - df\sqrt{dp + V_i}\right)$$

therefore

$$(58) \qquad g_i - g_j = gf\,df\left(\sqrt{dp + V_j} - \sqrt{dp + V_i}\right)$$

and manipulating (58) for two pairs of biases, and forming the difference, gives

$$(59) \qquad \frac{\sqrt{dp + V_2} - \sqrt{dp + V_1}}{g_1 - g_2} - \frac{\sqrt{dp + V_3} - \sqrt{dp + V_1}}{g_1 - g_3} = 0 \,.$$

Starting with an initial estimate of $dp = 2$, (59) can be solved using Newton-Raphson iteration. Then

$$(60) \qquad df = \frac{g_1 - g_3}{g_1\sqrt{dp + V_3} - g_3\sqrt{dp + V_1}}$$

and

$$(61) \qquad gf = \frac{g_1}{1 - df\sqrt{dp + V_1}} \,.$$

An alternative is to, assuming that the depletion pinching effect is small, initialize gf to g at the lowest (zero) V_i, set $dp = 2$, and then calculate an initial df from (57) at the highest V_i. A 3-dimensional Newton-Raphson iteration can then be used to solve for gf, df, and dp using (57) at the three V_i values.

A direct solution also exists. From (57)

$$(62) \qquad \frac{1}{df^2} + \frac{g_i^2}{df^2 gf^2} - \frac{2g_i}{df^2 gf} = dp + V_i$$

and forming the difference between this quantity for two combinations of the selected three bias points gives

$$(63) \qquad \begin{bmatrix} g_1^2 - g_2^2 & 2(g_2 - g_1) \\ g_1^2 - g_3^2 & 2(g_3 - g_1) \end{bmatrix} \begin{bmatrix} p_1 \\ p_2 \end{bmatrix} = \begin{bmatrix} V_1 - V_2 \\ V_1 - V_3 \end{bmatrix}$$

where $p_1 = 1/df^2 gf^2$ and $p_2 = 1/df^2 gf$. These two quantities can be calculated from the V_i and g_i data using (63), then

$$(64) \qquad gf = p_2/p_1 ,$$

$$(65) \qquad df = 1/\sqrt{p_2 gf} ,$$

$$(66) \qquad dp = \frac{1}{df^2} + \frac{g_1^2}{df^2 gf^2} - \frac{2g_1}{df^2 gf} - V_i .$$

The nonlinearity from the depletion pinching has the greatest sensitivity to dp for small V_i, therefore one bias should be at as small a V as possible (zero, if small-signal conductance is being used as opposed to large signal conductance) and $V_{1c} = 0$. Preferably data should be taken for 3 or more V_{1c} values (including zero). If such data are available then the other points used for extraction should be at the smallest V_{ds} and the second lowest V_{1c}, and the smallest V and the highest V_{1c}. If data for only two V_{1c} values (including zero) are available, besides the lowest V and lowest V_{1c} point, use the lowest V_{1c} point with a V higher than the smallest value and both small enough to ensure self-heating and velocity saturation effects are negligible and large enough to be sufficiently different from the lowest V value (so as not to be sensitive to measurement noise), and again as a third bias use the smallest V and the highest V_{1c} point.

For poly resistors, the "pinching" effect is from the depletion region at the bottom of the resistor, and from [3] the conductance of a poly resistor is

$$(67) \qquad g = \frac{XW}{\rho L} \left(1 - \frac{k_{Si} T_{ox}}{k_{ox} X \sqrt{V_0}} \sqrt{V_0 + 2V_{1c}} \right)$$

where X, W, and L are the thickness, width, and length of the polysilicon film that makes up the resistor, k_{Si} and k_{ox} are the relative dielectric permittivities of silicon and silicon dioxide, T_{ox} is the oxide thickness, ρ is the resistivity, and $V_0 = q\varepsilon_{Si} N/C_{ox}^2$. This can be seen to have the same general form as (1), which is why the basic depletion pinching bias dependence of the r3_cmc model is also, with appropriate parameters, suitable for modeling poly resistors.

For typical poly resistors on relatively thick oxides the V_0 of (67), which can be identified as the dp of (1), is large, several tens or hundreds of volts, compared to the 1-2V value (twice the built-in potential) for dp of a typical diffused resistor. Therefore the resistor conductance is

(68) $\qquad g \approx gf\left(1 - df\sqrt{dp} - df\,V_{1c}/\sqrt{dp}\right).$

which, as measured data also shows, has a linear $g(V_{1c})$ dependence. This means that there are only two independent quantities that can be extracted from measured data, the zero-bias value $g_0 = gf\left(1 - df\sqrt{dp}\right)$ and the slope $s = -gf\,df/\sqrt{dp}$. Yet there are three parameters for the model. Physical quantities are needed to break this indeterminacy. From [3] the value of $dp = V_0 = q\varepsilon_{Si}N/C_{ox}^2$ can be calculated; however because of incomplete dopant activation this can overestimate its value. It is better to calculate it from the poly sheet resistance,

(69) $\qquad dp = \dfrac{\varepsilon_{Si}T_{ox}^2}{\mu_0 X\rho_s \varepsilon_{ox}^2}$

where μ_0 and ρ_s are the low field mobility and sheet resistance of the poly, respectively. Therefore from the slope and zero-bias conductance

(70) $\qquad df = -\dfrac{s\sqrt{dp}}{g_0 - s\sqrt{dp}}$

and

(71) $\qquad gf = \dfrac{g_0}{1 - df\sqrt{dp}}.$

Calculating large signal conductance $g = I/V$ for small V can be problematic; V needs to be small enough so that self-heating and velocity saturation effects do not affect the device, but large enough so that g can be calculated reliably. For poly resistors, there is an alternative method to characterize the depletion pinching parameters. If $V_{1c} = 0$, and V is swept from a negative to a positive value (this is not possible for diffused resistors, as the parasitic junction diodes would become forward biased), then the conductance $g(V)$ has a roughly parabolic shape near $V = 0$. For poly resistors with negative temperature coefficients of resistance, the conductance increases (from self-heating) as the magnitude of the applied V bias increases (for sufficiently high V the conductance starts to decrease from velocity saturation, leading to a "horned" characteristic in the plot). If the temperature coefficient of resistance is positive, then the conductance will decrease as V increases (in roughly the same manner as the effect of velocity saturation, which makes them difficult to distinguish, without including additional data such as the frequency dependence of the output conductance).

For some magnitude of applied V, of both positive and negative signs, the effects of velocity saturation and self-heating should be the same (with the difference noted below). Therefore the plot of $g(V)$ should, to first order, be symmetric about $V = 0$. However because the V_{2c} bias differs between the positive and negative V cases, the amount of depletion pinching is different, and this introduces a slight asymmetry in the characteristic. (If the currents differ then so will the self-heating, but this should be a second order effect and so is ignored here). Because the effects of velocity saturation and self-heating affect the zero bias conductance and the mobility reduction parts of the model, the ratio of the magnitudes of currents with positive and negative V of equal magnitude cancel these

$$(72) \qquad \frac{I_p}{I_m} = \frac{I(+V)}{I(-V)}\bigg|_{V_{c1}=0} = \frac{1-df\sqrt{dp+V}}{1-df\sqrt{dp-V}} \approx 1-df^2 dp - V\frac{df}{\sqrt{dp}}$$

and therefore reveal the effect of depletion pinching. As with the low V bias analysis above, dp can be calculated from (69) and then df, or at least in initial value of it for optimization, can be determined from the slope of the ratio (72) versus V (once it stabilizes, the ratio tends to be "noisy" for low V).

For poly resistors where self-heating dominates the non-linearity, at low V the $g(V)$ parabolic shape is primarily determined from mobility reduction due to self-heating, therefore [2]

$$(73) \qquad \frac{g(V)}{g(0)} = 1 + \frac{T_{C1}}{\texttt{gtha}\cdot\texttt{rsh}}\left(\frac{V}{L}\right)^2$$

allows $\texttt{gtha}$ to be estimated.

One other recommendation is that one basic goal of the model is to model the deviation from linearity (which is important for distortion modeling), and to extract model parameters from that [8].

Because of local variation (mismatch) it can be difficult to merge data from different devices for model parameter extraction. Therefore extraction from individual devices can be beneficial. Modeling the deviation from linearity for individual devices does both of these.

14 References

[1] R. V. H. Booth and C. C. McAndrew, "A 3-Terminal Model for Diffused and Ion-Implanted Resistors," *IEEE Trans. Electron Dev.*, vol. 44, no. 5, pp. 809-814, May 1997.

[2] C. C. McAndrew, "R3, an Accurate JFET and 3-Terminal Diffused Resistor Model," *Proc. Nanotech WCM*, vol. 2, pp. 86-89, 2004.

[3] J. Victory, C. C. McAndrew, J. Hall, and M. Zunino, "A 4-Terminal Compact Model for High Voltage Diffused Resistors with Field Plates," *IEEE J. Solid-State Circuits*, vol. 33, no. 9, pp. 1453-1458, Sep. 1998.

[4] C. C. McAndrew, S. Sekine, A. Cassagnes, and Z. Wu, "Physically Based Effective Width Modeling of MOSFETs and Diffused Resistors," *Proc. IEEE ICMTS*, pp. 169-174, 2000.

[5] R. Brederlow, W. Weber, C. Dahl, D. Schmitt-Landsiedel, and R. Thewes, "A physically based model for low-frequency noise of poly-silicon resistors," *Tech. Digest IEDM*, pp. 89-92, 1998.

[6] C. C. McAndrew, G. Coram, A. Blaum, and O. Pilloud, "Correlated noise modeling and simulation," *Proc. NanoTech WCM*, pp. 40-45, 2005.

[7] "r2_cmc: Two-Terminal   Nonlinear   Resistor   Model,"   available   at http://www.eigroup.org/cmc/downloads/r2_cmc/r2_cmc_v1.0_r0.0_2005nov12.pdf

[8] P. Humphries, CMC Meeting, Dec. 2006.